

2.3

Towards Fully Automated Verification of Semiconductor Technologies

Matthias Ludwig¹, Dinu Purice², Bernhard Lippmann¹,
Ann-Christin Bette¹ and Claus Lenz²

¹Infineon Technologies AG, Munich, Germany

²Cognition Factory GmbH, Munich, Germany

Abstract

In an ever more connected world, semiconductor devices are at the heart of every technically sophisticated system. Safety and security in operation, on which many times vital personal or business data or our lives depend on, is critical. The market for semiconductors is tremendous, and rogues also to get their share by selling counterfeit products which potentially jeopardize that very safety and security. Trust into semiconductor devices can be created by securing the supply chain or by verifying the electrical characteristics, the physical layout and the manufacturing technology against the design and specifications. The objective of this work is to propose a verification pipeline for semiconductor devices utilizing their technological features computed by the means of an automated device cross-section analysis. The emphasis lies on the confluence of an established industrial analytic process with novel possibilities provided by the advances in data processing and machine learning. This framework, its technical implementations, and exemplary results of our proposed autonomous technology analytics approach are presented in this work. Furthermore, the results are compared against a manual expert's measurement which underline the high performance of the framework and its effective multi-stage realisation.

Keywords: industrial artificial intelligence, failure analysis, anti-counterfeiting, hardware trust, verification and validation, semiconductor technology analysis, image processing, convolutional neural network, semantic segmentation, pattern recognition, supervised learning, deep learning.

2.3.1 Introduction

Trust into microelectronics [2], [3] can be generated by the validation and verification [12] of its originality. With today's world-wide distributed supply chains of microelectronics manufacturing, validating the safety, security, and trustworthiness of these devices is a highly complex task. Still, it is of paramount importance: electronics span every aspect of our daily lives and range from applications such as the (industrial) internet of things, over consumer electronics, to connected vehicles.

A way to check a product's originality is through physical inspection techniques, such as cross-sectioning. Through a sub-sequent analysis of the cross-sections, the integrity of the manufacturing technology [11] can be verified. To achieve this, all technological properties can be used in a verification process. In the case of cross sections, these are geometric shapes and dimensions, or material-related properties. Each technology can be interpreted as a unique fingerprint, so that deviations from specifications can be reported as suspicious. Nonetheless, physical inspection techniques must keep up with the continuously growing complexity of advanced semiconductor manufacturing nodes, and automation is another requirement in demand.

Cross-section (CS) images from scanning electron microscopes (SEM) are acquired at the failure analysis or process control labs and are a standard analysis process in the semiconductor industry. By the usage of SEM-integrated software tools, the technological features are manually measured and evaluated by engineers. Due to the expenditure of human labour, this process is costly and domain knowledge is required to fully interpret a sample or to detect anomalies in a set of images. The data is already available today, with datasets being produced at the sites. The utilization of data intensive analysis methods opens the possibility to create additional value by saving analysis expenses - and in the end overall cost - with an automated interpretation and measurement approach.

Figure 2.3.1 shows the second important aspect of the inspection flow: the full abstraction stack – ranging from software applications down to the

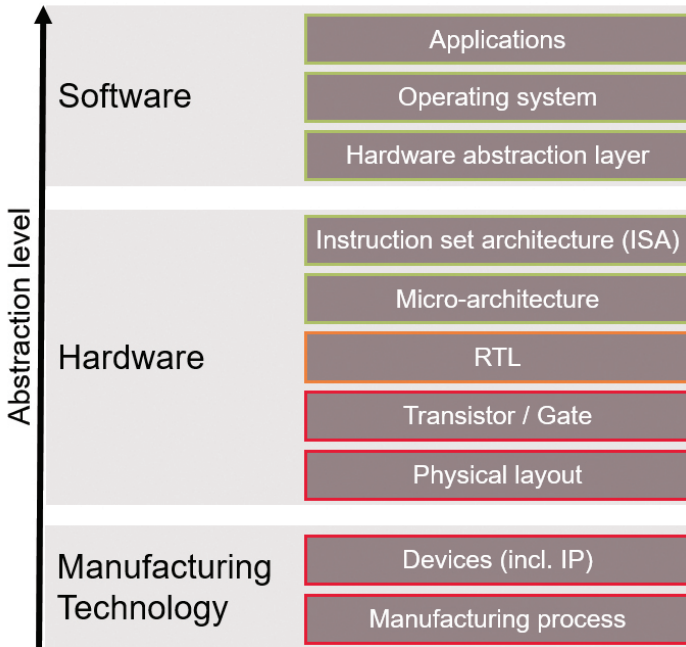


Figure 2.3.1 Abstraction layers in typical computing systems, ranging from software, over hardware design, to the underlying manufacturing technology.

physical implementation – of complex computing systems is illustrated. More and more software layers and manufacturing technology-agnostic layers can be investigated through published methods for verification of security [4] and functional safety (IEC 61508). Yet, the lower layers remain proprietary with no way to verify the integrity of their design. There have been several publications addressing the integrity checking of physical properties of semiconductor packages [5], [6], [7], and supply chain security related approaches [8]. Summaries about the detection and avoidance schemes of counterfeit electronics can be found in [1], [9], [10]. This work aims to push the boundaries of the state-of-the-art of automated physical inspection by the enablement of an automated detection of suspicious devices through SEM cross-section analysis.

In this work, academic and industrially relevant topics are discussed: First, the technology related characteristic – providing methods to secure the integrity of integrated devices. And second, the implementation of an industrial automation use-case – integrated into a complex established

environment – which can be seen paradigmatic for the challenges and possibilities of the entire project.

2.3.2 Background: Interpreting Semiconductor Technologies

The tremendous manufacturing improvements of past years and decades for semiconductor devices are shown in Figure 2.3.2. The CS images show four different technology *stacks*, from 150nm (introduced in the early 2000s) down to a more advanced 28nm (introduced in the early 2010s) process node. On these equally scaled CS images it is shown that the size of critical dimensions (CDs) has been continuously shrunk. On the other hand, the total number of processing steps and subsequently the number of visible objects is increasing.

The *stacks* visible in the images can be interpreted as a unique fingerprint for each manufacturing technology and its measured properties allow an inference to the specified and designed technological features. Specifically from these images, the thickness for each deposited layer and the minimum dimensions of each lithographic pattern found for each layer can be extracted. The set of identified technological parameters then enables the identification of production technologies. The innovative novelty of our approach can be explained via Figure 2.3.3: In the current reverse engineering process, the input is a known or unknown device, with the target to analyse its physical properties (geometrical and material-related) and consequently its manufacturing process.

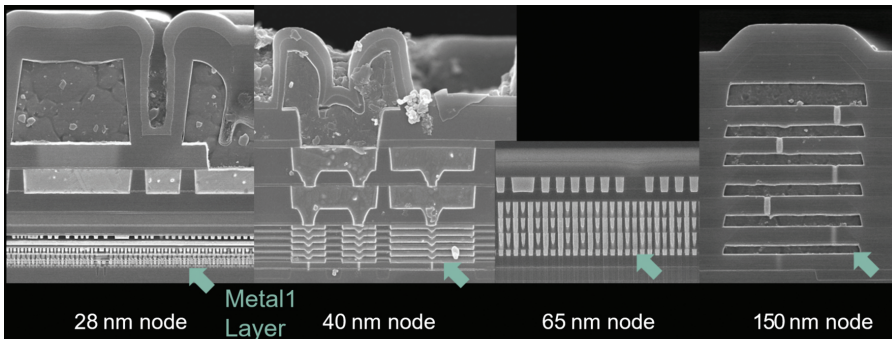


Figure 2.3.2 Equally scaled scanning electron microscope images of semiconductor device cross-sections, showing a 28nm, a 40nm, a 65nm, and 150nm process node (from [12]).

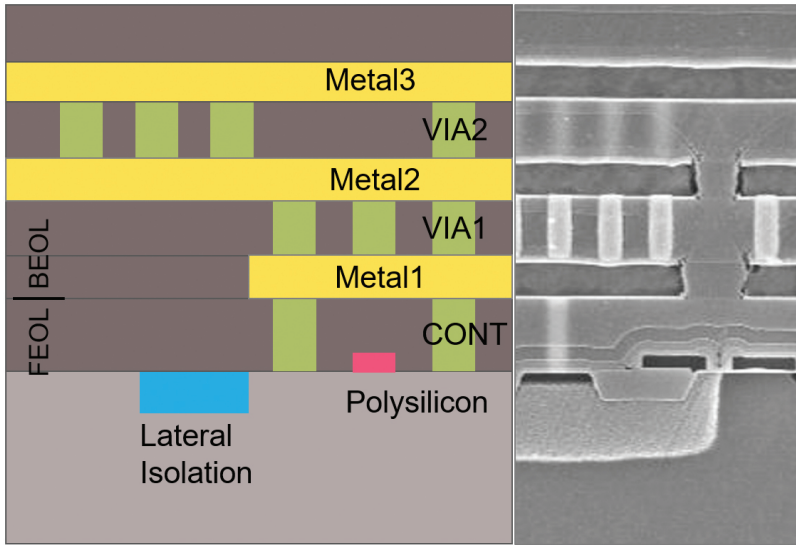


Figure 2.3.3 Example of a cross-section image which shows already interpreted objects on the left side and part of the raw image on the right side.

The application of the aforementioned principles for the purpose of counterfeit identification is even more challenging when vast numbers of features must be correlated and interpreted against known technology definitions. An automated processing of this data has been enabled by the advances in image processing and automated feature extraction.

The integration of technology domain knowledge and AI methods into a well-controlled industrial process (see Figure 2.3.4) is a fundamental prerequisite of the project. Considering the challenges of a supervised deep learning approach to interpret the SEM images, contributions from both fields were needed to produce the labelled dataset. Yet due to the high complexity of the task and the non-availability of methods to analyse the complex data structures, it was not possible to provide a fully automated approach. This missing link between AI methods and domain knowledge and the use cases is worked out by the proposed approach of SEM image interpretation and presented in this work. The second stage of overlap between the application and AI fields then comes into play during the segmentation result interpretation process. During this process, the segmentation accuracy does not linearly translate into overall technology prediction accuracy. This is explained by the fact that certain features identified by the deep learning (DL)

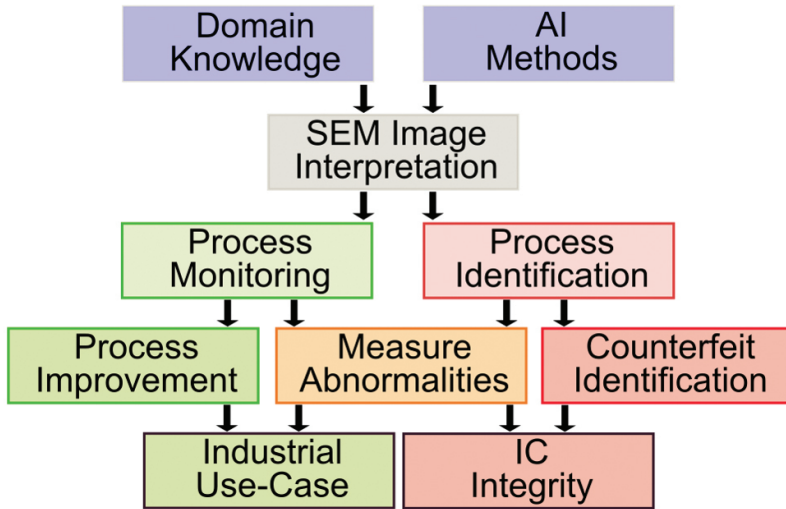


Figure 2.3.4 Overall framework of the project. Domain knowledge and AI methods were the enabler for the use-cases that are facilitated through the automated SEM image interpretation.

methodology have a larger impact on subsequent calculation than others. Consequently, a looped, iterative development approach was followed to ensure the AI component of the overall process is trained adequately. An emphasis is put on the most relevant and critical features, instead of the more common approach of maximizing a pre-defined accuracy metric.

2.3.2.1 Methodology: The Integrated Analysis Process

A conspectus of the whole analysis process is shown in Table 2.3.1, where the established laboratory process is extended via two software (data processing) steps. The entire process is outlined in detail in this chapter.

Table 2.3.1 Framework of the cross-section interpretation with the respective sub-processes.

	Sub-Process	Sub-Steps	Intermediate Results
Process Flow ↓	Lab work	Established analysis process: <ul style="list-style-type: none"> • Physical sample preparation • SEM image acquisition 	Grey-scaled images
	Feature extraction	<ul style="list-style-type: none"> • Image segmentation • Object vectorisation 	Vectorised images, objects per class
	Feature processing	<ul style="list-style-type: none"> • Feature measurement • Technology determination 	Technology features, technology platform

Sample preparation and image acquisition: Even though cross-sectioning is considered a standard process, mastering the physical process can take several years. Two main methods for cross-sectioning exist: The first is a deposition of the sample in epoxy and subsequently an abrasive grinding of it. Moreover, the cross-sectioning can be performed on a glass grinding wheel, after devices package has been detached. The last step in the laboratory is the image acquisition via SEMs [13].

Image Processing: The goal of the image processing step is to provide fast, reliable, and accurate segmentations based on SEM images. The images are grey-valued with ambiguous intensity values for different object classes, as indicated in Figure 2.3.5. Furthermore, the task difficulty is boosted by the various zoom levels and variability of the regions of interest sizes.

The overlaps between different classes represented in Figure 2.3.5. A challenge the use of classical computer vision segmentation techniques such as thresholding, region-growing, or histogram-based methods. Nevertheless, these approaches are useful to supplement the segmentation pipeline in pre- and post-processing steps. The nature of the SEM images bears high similarity to medical images, particularly computed tomography and magnetic resonance images, where AI based techniques are becoming increasingly investigated to solve segmentation challenges. Therefore, a set of experiments aimed at comparing various DL state-of-the-art fully convolutional methods were conducted, comparing architectures such as U-net [15], PSPNet [18], FPN [19], GSCNN [20], Siamese-based [23]. It is concluded that overly complex architectures overfit specific tasks and often underperform on high-variance data, and while being commonly used as a benchmark, the U-net basis for the CNN architecture can outperform

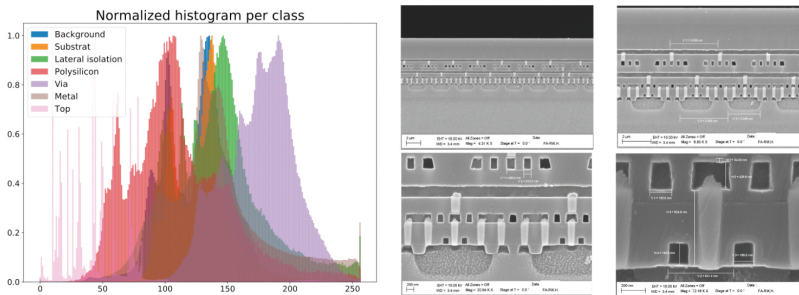


Figure 2.3.5 A. Normalized histogram per class. B. Various zoom levels of the same image, magnified 4310, 8650, 20940 and 72180 times, respectively.

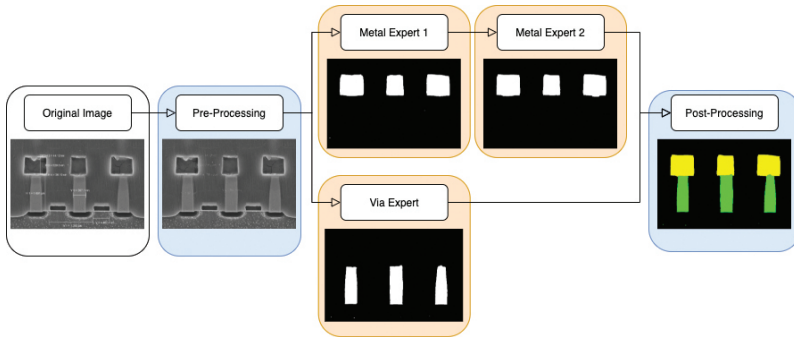


Figure 2.3.6 Exemplified overview of the segmentation pipeline.

other architectures assuming proper pre- and post-processing techniques [14]. Subsequently, a cascade U-net based architecture is concluded to be most suitable for the task at hand.

A dataset of around 500 images was created and labelled in pixel-wise accuracy, and dedicated networks were trained for metal and VIA (vertical interconnection access) segmentation (further called “experts”). First level experts segment the down-sampled image, and pass the resulting segmentation (one-hot encoded) to the second level expert along with the input image, who produces a more accurate output, much less vulnerable to outliers. Due to the varied nature of the labels of interest it was concluded that such a cascaded approach is beneficial for metal segmentation, while providing negligible improvements for VIAs, which were subsequently segmented by a single “expert”.

The issue of the relatively small dataset was tackled using image augmentation including horizontal flips and small rotations. Segmentation problems involving high intra- and inter-class imbalance (as is the case in question) have shown to be solved most successfully using Dice-based loss functions [16]. Therefore, several candidates were investigated as hyper-parameter options, with metal segmentation benefitting most from LogCoshDSC Loss [22], and VIA segmentation from Focal Tversky Loss [21], respectively. The high number of hyperparameters were tuned using a population-based approach. The evolutionary nature of the approach ensured high confidence in the obtained parameters and better final performance while keeping computational time requirements within reasonable limits [17]. The obtained results yield a 24 % increase in accuracy compared to the baseline version, and obtained an overall Dice score of 0.90. Examples of resulting segmentations are presented below in Figure 2.3.7.

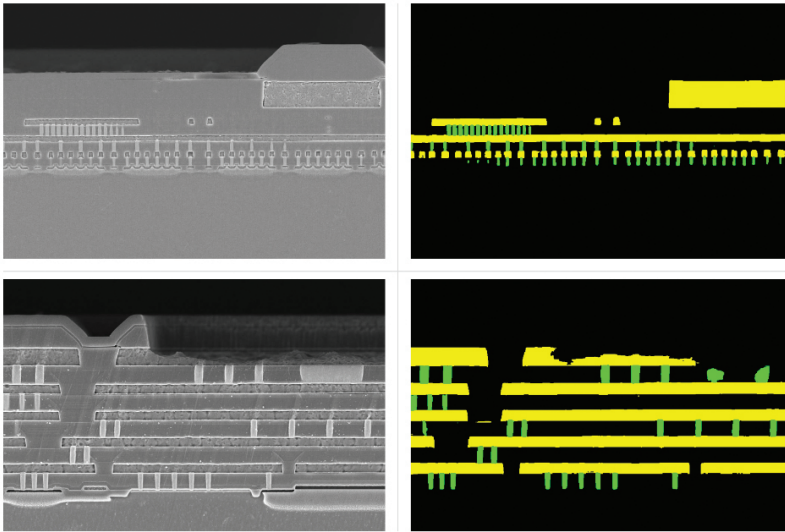


Figure 2.3.7 Examples of segmented images with yellow illustrating metal components, and green illustrating VIAs.

Image Measurement: The segmented images are calibrated via SEM meta-data or pattern matching of the dimensional bars and then vectorised into polygons of the different classes (e.g.: metal, VIAs, etc.). Polygons enable the utilization of their inherent attributes like the centroid, the circumference, or the area. An innovative – completely unsupervised - usage of these attributes is used for pattern recognition purposes. Established clustering methods [24] are linked with the properties of manufactured semiconductor devices. From these clusters the geometrical features are determined.

Technology Determination: The target is to evaluate the correct technology platform via the computed process feature vector. This vector will have dozens of measured attributes which are correlated against the known technology definitions (see example in Figure 2.3.8). In our implementation, distance metrics (Euclidean, rectilinear distance) between measured and defined values have been shown to yield good prediction results. A further improvement will be gained through assessment of individual feature importance by variable selection techniques.

In the example in Figure 2.3.8, three random features – metal 1 thickness, contact height, contact minimum pitch, and the total number of metal layers (colour coded) – are plotted for several dozen possible technology

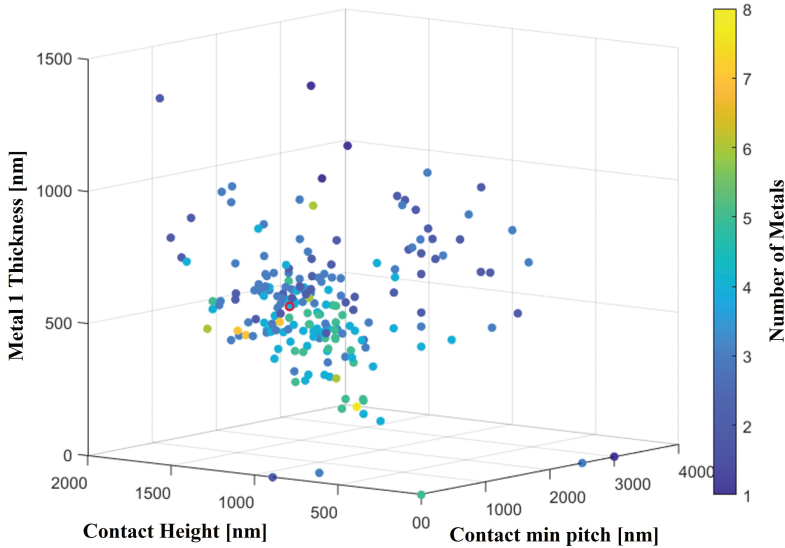


Figure 2.3.8 Example features of different semiconductor technologies. The four dimensions were arbitrarily chosen from more than hundred possible attributes defining a semiconductor front-end technology.

specifications. These characteristics are also of importance for a correct determination. The red mark shows an example measurement and the closest distance to adjacent data-points yields the most likely technology match. These three dimensions are extended to a higher dimensional space in the application.

2.3.2.2 Example Analysis: From the Image to the Feature Extraction

To conclude our work, the technological attributes of the VIAs of a sample are extracted. The VIAs are shown in the grey-scale image of Figure 2.3.9 and indicated through red boxes. After their semantic segmentation, the VIA objects appear in green and the metal lines in yellow. A visual inspection shows that all VIAs have been neatly extracted. The same applies to the metal, except for the top metal which shows a minor tear in the middle section. The measurement of the geometrical features (pitch and height) is shown in Table 2.3.2 and the automated measurement is compared against the manual measurement of an expert operator. The deviation on the right column shows the feasibility of an autonomous analysis which can also be done with

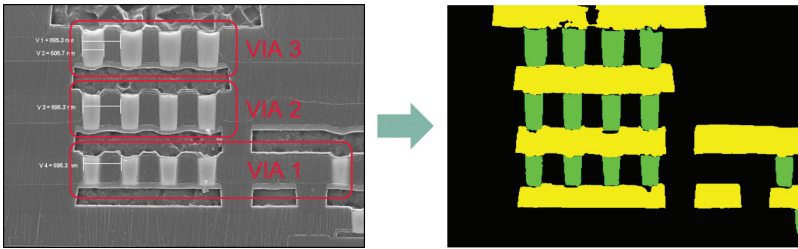


Figure 2.3.9 Example SEM CS with the grey-scaled SEM image (left) and the segmented image (right).

Table 2.3.2 Results of measured features of the VIAs. In the right column, the deviation between the automated and the manual is shown.

Measurement	Auto	Manual	Dev. [%]
VIA 1 Pitch [nm]	917	895	2.4
VIA 1 Height [nm]	675	711	5.1
VIA 2 Pitch [nm]	912	895	1.9
VIA 2 Height [nm]	700	742	5.7
VIA 3 Pitch [nm]	910	895	1.7
VIA 3 Height [nm]	779	806	3.3

other measurable features. Due to the high accuracy of the measurement, the technology platform determination for this example was successful.

2.3.3 Conclusion

The possibility of applying state-of-the-art AI approaches has enabled us to extend the existing workflow by an automated technology analysis. It has been shown that an extraction of technological attributes from SEM CS images in a fully autonomous manner is possible, with results comparable to an operator's manual effort. The most challenging part was the confluence of the knowledge of both domain experts and AI/ML experts.

The presented framework allows an automated check of the inferred technological parameters for verification and validation against specifications. Additionally, emphasis is put on a modular design of the sub-tools. This allows a migration to other applications and an extension of the presented status with other classes for segmentation is not overly complex. In summary, this contribution is a steps towards improved physical inspection for hardware assurance. A future task will be the application of the framework on real world examples.

Acknowledgements

This work is conducted under the framework of the ECSEL AI4DI “Artificial Intelligence for Digitising Industry” project. The project has received funding from the ECSEL Joint Undertaking (JU) under grant agreement No 826060. The JU receives support from the European Union’s Horizon 2020 research and innovation programme and Germany, Austria, Czech Republic, Italy, Latvia, Belgium, Lithuania, France, Greece, Finland, Norway.

References

- [1] U. Guin, K. Huang, D. DiMase, J. M. Carulli, M. Tehranipoor, and Y. Makris, “Counterfeit integrated circuits: A rising threat in the global semiconductor supply chain,” *Proceedings of the IEEE*, vol. 102, no. 8, pp. 1207–1228, 2014.
- [2] T. Hoque, P. SLPSK, and S. Bhunia, “Trust issues in microelectronics: The concerns and the countermeasures,” *IEEE Consumer Electronics Magazine*, vol. 9, no. 6, pp. 72–83, 2020.
- [3] B. Liu, Y. Jin, and G. Qu, “Hardware design and verification techniques for supply chain risk mitigation,” in *2015 14th International Conference on Computer-Aided Design and Computer Graphics (CAD/Graphics)*, 2015, pp. 238–239.
- [4] O. Demir, W. Xiong, F. Zaghoul, and J. Szefer, “Survey of approaches for security verification of hardware/software systems.” *IACR Cryptology ePrint Archive*, vol. 2016, p. 846, 2016. <http://dblp.uni-trier.de/db/journals/iacr/iacr2016.html>
- [5] P. Ghosh and R. S. Chakraborty, “Recycled and remarked counterfeit integrated circuit detection by image-processing-based package texture and indent analysis,” *IEEE Transactions on Industrial Informatics*, vol. 15, no. 4, pp. 1966–1974, 2019.
- [6] R. Hammond. Counterfeit electronic component detection. ERAI, Inc. [Online]. Available: <https://www.aeri.com/counterfeit-electronic-component-detection/>
- [7] A. Kanovsky, P. Spanik, and M. Frivaldsky, “Detection of electronic counterfeit components,” in *2015 16th International Scientific Conference on Electric Power Engineering (EPE)*, 2015, pp. 701–705.
- [8] C. E. Shearon, “A practical way to limit counterfeits,” in *2019 Pan Pacific Microelectronics Symposium (Pan Pacific)*, 2019, pp. 1–7.

- [9] G. Caswell, "Counterfeit detection strategies: When to do it / how to do it," International Symposium on Microelectronics: FALL 2010, vol. Vol. 2010, no. No. 1, pp. 227–233, 2010.
- [10] M. M. Tehranipoor, U. Guin, and D. Forte, Counterfeit Integrated Circuits: Detection and Avoidance. Springer Publishing Company, Incorporated, 2015.
- [11] Y. Nishi and R. Doering, Handbook of Semiconductor Manufacturing Technology. CRC Press, 2017. <https://books.google.de/books?id=PsVVKzhjBgC>
- [12] B. Lippmann, N. Unverricht, A. Singla, M. Ludwig, M. Werner, P. Egger, A. Duebotzky, H. Graeb, H. Gieser, M. Rasche, and O. Kellermann, "Verification of physical designs using an integrated reverse engineering flow for nanoscale technologies," Integration, vol. 71, pp. 11 – 29, 2020. <http://www.sciencedirect.com/science/article/pii/S0167926019302998>
- [13] M. Vogel, Handbook of Charged Particle Optics, 2nd ed., J. Orloff, Ed. Contemporary Physics, 2010, vol. 51, no. 4.
- [14] Isensee, F., Petersen, J., Klein, A., Zimmerer, D., Jaeger, P. F., Kohl, S., Wasserthal, J., Koehler, G., Norajitra, T., Wirkert, S., & Maier-Hein, K. H. (2018). nnU-Net: Self-adapting Framework for U-Net-Based Medical Image Segmentation. Informatik Aktuell, 22. <http://arxiv.org/abs/1809.10486>
- [15] Ronneberger, O., Fischer, P., & Brox, T. (2015). U-Net: Convolutional Networks for Biomedical Image Segmentation. In Lecture Notes in Computer Science (including subseries Lecture Notes in Artificial Intelligence and Lecture Notes in Bioinformatics) (Vol. 9351, pp. 234–241). https://doi.org/10.1007/978-3-319-24574-4_28
- [16] Milletari, F., Navab, N., & Ahmadi, S.-A. (2016). V-Net: Fully Convolutional Neural Networks for Volumetric Medical Image Segmentation. 2016 Fourth International Conference on 3D Vision (3DV), 565–571. <https://doi.org/10.1109/3DV.2016.79>
- [17] Jaderberg, M., Dalibard, V., Osindero, S., Czarnecki, W. M., Donahue, J., Razavi, A., Vinyals, O., Green, T., Dunning, I., Simonyan, K., Fernando, C., & Kavukcuoglu, K. (2017). Population Based Training of Neural Networks. <http://arxiv.org/abs/1711.09846>
- [18] Zhao, H., Shi, J., Qi, X., Wang, X., & Jia, J. (2017). Pyramid scene parsing network. Proceedings - 30th IEEE Conference on Computer Vision and Pattern Recognition, CVPR 2017, 2017-Janua, 6230–6239. <https://doi.org/10.1109/CVPR.2017.660>

- [19] Li, X., Lai, T., Wang, S., Chen, Q., Yang, C., & Chen, R. (2019). Weighted feature pyramid networks for object detection. Proceedings - 2019 IEEE Intl Conf on Parallel and Distributed Processing with Applications, Big Data and Cloud Computing, Sustainable Computing and Communications, Social Computing and Networking, ISPA/BDCLOUD/SustainCom/SocialCom 2019, 1500–1504. <https://doi.org/10.1109/ISPA-BDCLOUD-SustainCom-SocialCom48970.2019.00217>
- [20] Takikawa, T., Acuna, D., Jampani, V., & Fidler, S. (2019). Gated-SCNN: Gated shape CNNs for semantic segmentation. In Proceedings of the IEEE International Conference on Computer Vision (Vols. 2019-October). <https://doi.org/10.1109/ICCV.2019.00533>
- [21] Abraham, N., & Khan, N. M. (2019). A novel focal tversky loss function with improved attention u-net for lesion segmentation. Proceedings - International Symposium on Biomedical Imaging, 2019-April, 683–687. <https://doi.org/10.1109/ISBI.2019.8759329>
- [22] Yeung, M., Sala, E., Schönlieb, C.-B., & Rundo, L. (2021). A Mixed Focal Loss Function for Handling Class Imbalanced Medical Image Segmentation. <http://arxiv.org/abs/2102.04525>
- [23] Martin, K., Windunga, N., Sani, S., Massie, S., & Clos, J. (2017). A convolutional siamese network for developing similarity knowledge in the SelfBACK dataset. CEUR Workshop Proceedings. <https://rgu-repository.worktribe.com/output/246838/a-convolutional-siamese-network-for-developing-similarity-knowledge-in-the-selfback-dataset>
- [24] S. Wierzchon and M. Kłopotek, “Modern algorithms of cluster analysis,” Springer International Publishing, vol. 34, 01 2018.